

PULSED POWER FUEL CELLS

R. A. Sanderson, C. L. Bushnell, T. F. McKiernan

Pratt & Whitney Aircraft Division
United Aircraft Corporation
East Hartford, Connecticut

INTRODUCTION

Fuel cells are presently under development for a variety of applications. Hydrogen-Oxygen fuel cells were used in the Gemini Space Program and are now part of the Apollo Space Program. Fuel cells operating on preconditioned hydrocarbon fuels and air are also being developed in a variety of military and commercial programs as high efficiency electrical power supplies.

In these programs, the fuel cells are primarily subjected to steady direct current loading at relatively low power density, less than 300 watts per square foot of electrode area.

Fuel cell operation at high current density under pulsed loading was the subject of a recent program at Pratt & Whitney Aircraft. This work was sponsored by the Air Force Aero Propulsion Laboratory at Wright-Patterson Air Force Base. The object of the program was to investigate fuel cells as a source of short duration high intensity electrical discharge in the microsecond to 5 minute discharge time range.

This paper describes fuel cell performance characteristics noted during this investigation, including microsecond response following a single switch closure and the response to repeated square wave pulse loadings over a range of pulse frequency and pulse duration.

CELL PERFORMANCE CHARACTERISTICS

Figure 1 shows a typical fuel cell steady-state performance characteristic. If the cell is operating at a given point on the steady-state curve, then the voltage at the cell terminals is given by:

$$E_{oc} - E_p = IR$$

Where:

- E_p = $E_a + E_c + I(R_{in})$
- E_{oc} = open circuit voltage
- E_a = anode polarization
- E_c = cathode polarization
- I = cell current
- R_{in} = internal cell resistance
- E_p = total cell polarization
- V = operating voltage
- R = external circuit resistance

The left side of the above equation represents the difference between the cell open circuit voltage and the voltage at the operating point (V). This difference is the sum of the anode, cathode and internal polarizations of the cell. The external load line can be superimposed

upon the steady-state performance curve by connecting the origin and the operating point.

When the cell is initially at an open circuit condition and a load is applied, the load line changes from the initial value (slope = ∞) to the new value (slope = R). If the load is changed to this new value (slope = R) very slowly, the cell polarizations have sufficient time to develop, and the performance path follows along the steady-state characteristic A to C. If the load is changed rapidly, such as closing a switch, the performance path moves from A to B. Then, as the polarizations develop within the cell, the performance decays back to point C.

Tests were conducted at Pratt & Whitney Aircraft to investigate the performance path during switch closure.

TEST CIRCUIT

The circuit used to obtain fuel cell transient response is shown in Figure 2. Tests were generally conducted on cells with an active area of 0.5 in² to keep current in the electronic switch during repeated pulsing within the 50 amp rating of the transistors. In some of the single switch closure tests, a hand switch was substituted for the solid state electronic switch.

Connections between components in the circuit were made as short as possible to minimize inductance.

RESPONSE TO A SINGLE SWITCH CLOSURE

Initial tests were conducted on fuel cells using Pratt & Whitney Aircraft catalyzed screen type electrodes with the aqueous KOH electrolyte trapped in a 10 mil asbestos matrix. The tests were at 220°F with 15 psia H₂-O₂ reactants on 0.5 in² cells. Figure 3 shows voltage and current traces recorded from the oscilloscope following switch closure with minimum circuit resistance (later calculated at 0.0032 ohms).

The time scale is 50 microseconds per cm. The traces do not start at zero current and open circuit due to a delay in triggering the scope. Peak recorded current was approximately 55 amps (15,600 amps/ft²) at a cell voltage of 0.2 occurring about 100 microseconds after switch closure.

Figure 4 shows the same switch closure transient recorded at 10 milliseconds per cm. After 100 milliseconds the current is still above 8500 amps/ft².

During this step transient roughly 100 joules/ft² of energy was released (in 100 milliseconds), and the calculated capacitance of the cell was 280 farads/ft². Maximum output power density during this transient was 5900 watts/ft².

Figure 5 shows the switch closure transient plotted as voltage versus current. The normal steady-state performance is shown for comparison.

The calculated electrolyte resistance is also plotted on the voltage-current curve. It can be noted that current from the cell exceeded the maximum expected, based on the electrolyte loss indicating the overall cell is behaving as a capacitor with higher discharge currents through the external circuit than through the cell itself.

Tests were also performed using a dual pore nickel electrode cell in free electrolyte. These tests were conducted at 400°F with 85 weight percent KOH. The electrolyte gap between the cells was 0.060 inch.

During the switch closure test, current densities up to 5750 amps/ft² were recorded, as shown in Figure 6 (Trace A). Peak power density was 6240 watts/ft².

A second test was then made with a Teflon barrier placed in the electrolyte between the electrodes, blocking the electrodes but allowing ion flow around the edges. The cell was once again pulsed from open circuit as shown in Figure 6 (Trace B). Peak current was 5370 amps/ft², nearly the same as when tested without the ion barrier between the cells. Voltage and current dropped off at a faster rate in this test.

A third test was then made. With the cell at open circuit, the cell was withdrawn from the electrolyte leaving an air gap between the cells. The switch was then closed. Current densities up to 3600 amps/ft² were recorded as a measure of the cell's pure capacitance, Figure 6 (Trace C). Voltage and current dropped off very rapidly as the cell discharged without the advantage of recharge current in the cell.

Calculated capacitance for the three tests was:

1. Normal configuration 0.060 inch free electrolyte	550 farads/ft ²
2. With Teflon barrier between electrodes	314 farads/ft ²
3. With air gap between electrodes	19 farads/ft ²

Figure 7 shows voltage versus current curves for the three tests as well as the steady-state performance and the calculated maximum current based on electrolyte resistance.

Several trends were noted from these tests of cell response to a single switch closure:

1. Initial performance during step increases in load exceeds steady state due to cell capacitance. Peak current is limited by cell impedance during this initial period and the external circuit resistance.
2. Initial performance during step increases in load also exceeds the level predicted on the basis of pure resistance loss through the electrolyte. This can occur only if current through the external circuit exceeds ion current through the electrolyte.
3. Impedance during the initial time after switch closure is not limited by IR loss through the electrolyte but depends instead on the overall cell capacitance and resistive losses within the electrodes as well as current collection losses.
4. Capacitance of the cell increases with increasing electrode pore surface (electrode thickness, porosity). Cells with thin screen electrodes had a generally lower capacitance (200 farads/ft²) than cells with thicker electrodes such as the dual porosity free electrolyte cell (500-700 farads/ft²).

REPEATED PULSE TESTS

Cell performance was also investigated for a continuous pulse load in which a switch is opened and closed continuously at high frequency. Loading of this type could be imposed on the fuel cell by an input chopper stage on a voltage regulator or inverter, or by a pulse width modulation type motor speed control.

Repeated pulse loading tests were performed on a screen electrode low temperature trapped electrolyte cell using an electronic switch and square wave pulse generator. A range of pulse frequency (10 to 10,000 cps), pulse duration (20 to 95 percent), and pulse amplitude (1400 to 3600 amps/ft²) was imposed on the cell. Voltage readings were taken from the oscilloscope during both the pulse on and off time.

Figure 8 shows an oscilloscope trace with typical response of the cell during repeated pulsing at one kilocycle and 90 percent pulse duration. During the switch off interval, the cell does not have time to recover, and the performance arrives at a quasi steady-state level.

Figure 9 shows performance during the pulse-ON portion of the cycle for a range of pulse durations. Data points are readings taken directly from the oscilloscope. Since the objective of the program was high power output, data was recorded primarily at higher currents.

The average power density was computed for square wave response by multiplying the power while the pulse is ON by the pulse duration. Figure 10 shows cell voltage while the pulse is ON, plotted against average power density. Steady-state power density is also shown. At a cell voltage of 0.75, the average power density in a pulsing mode at 90 percent pulse duration is twice the output with a continuous load (initial steady state).

The effect of pulse duration and frequency is shown in Figure 11. Average power density improves with decreasing frequency and peaks at 80-95 percent pulse duration.

The results of repeated pulse loading on a dual pore free electrolyte cell at 450°F are shown in Figure 12. Average performance while pulsing exceeded performance during continuous d. c. load for pulse durations above 50 percent.

Tests were also performed on an early experimental activated dual porosity nickel electrode cell with 1/4 inch free electrolyte at 160°F. Performance of the cell is shown in Figure 13. Although the general performance level was low, considerable improvement in performance was noted by operating the cell in a pulsing mode as shown.

Several trends were noted during these repeated pulse tests.

1. During repeated pulsing, the cell capacitance is charged during the open circuit periods and discharged during the closed circuit periods.
2. The voltage at which current is drawn from the cell during closed circuit conditions is considerably greater than if the cell were operated under a continuous d. c. load. As the pulse duration is increased, the performance falls off.
3. The integrated average performance in a pulsing mode can exceed steady state. The extent of performance improvement is affected by cell type, load level, pulse duration, and frequency.
4. In general, the integrated average performance improves with lower frequency (100-1000 cps) and higher pulse duration 80-95 percent. Improvement in cell performance by pulsing also appears to be greater at higher current density and in cells with a generally lower performance. Further investigation is needed to evaluate the effect of pulse loading on cell endurance.

SUMMARY

The electrochemical capacitance of fuel cells has been evaluated in single switch closure tests and found to be in the order of 200-700 farads/ft² of cell area depending on cell type. This capacitance gives a fuel cell the ability to deliver high intensity microsecond-millisecond discharges up to 16,000 amps/ft² and 6000 watts/ft².

During continuous fuel cell operation, cell capacitance can be used by repeated pulsing at higher frequency. The results of repeated pulse testing indicates performance improvements up to 100 percent in current density at equal cell voltage.

References

1. AFAPL-TR-67-40 Pulse Power Fuel Cell, May 1967

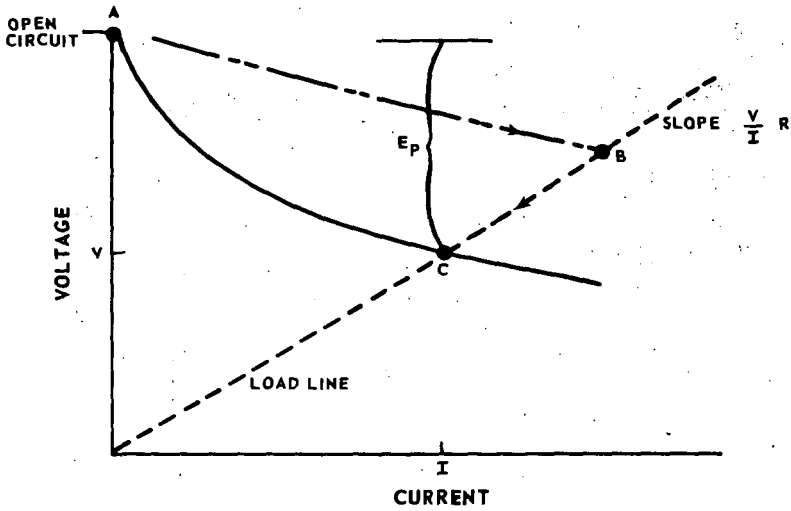


Figure 1 Fuel Cell and Load Characteristics

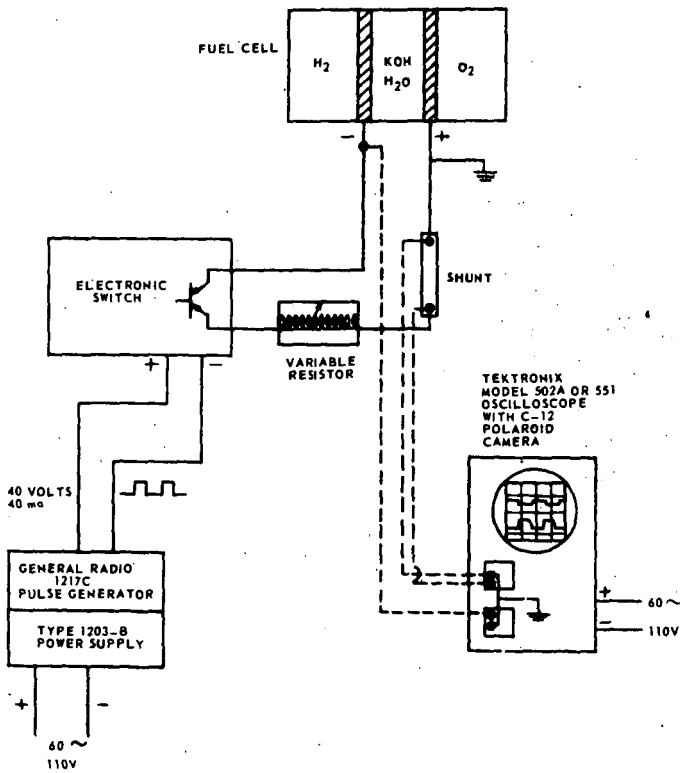


Figure 2 Circuit for Testing Fuel Cell Performance to Pulse Loads

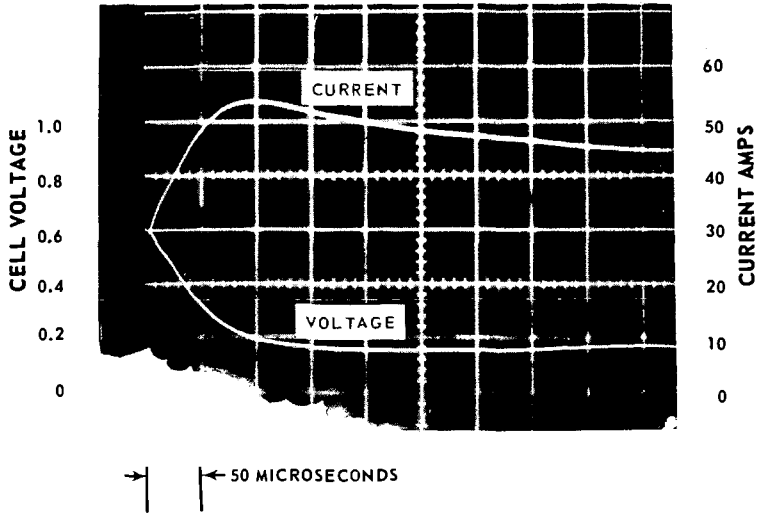


Figure 3 Trapped Electrolyte Cell Microsecond Response Following Switch Closure

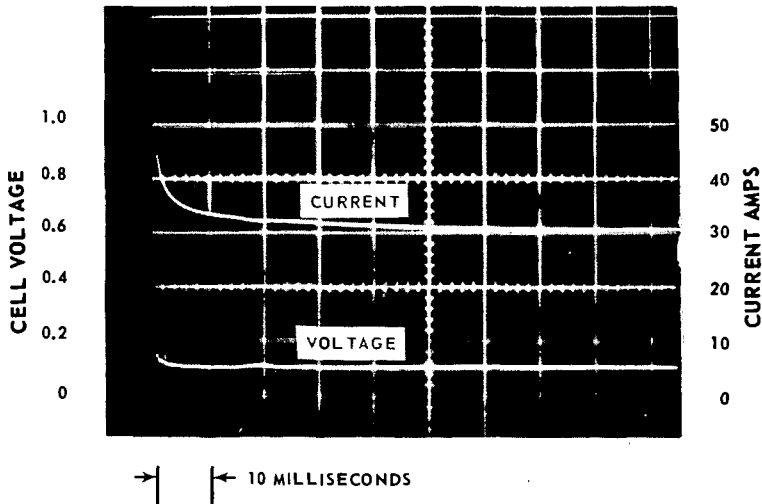


Figure 4 Trapped Electrolyte Cell Millisecond Response Following Switch Closure

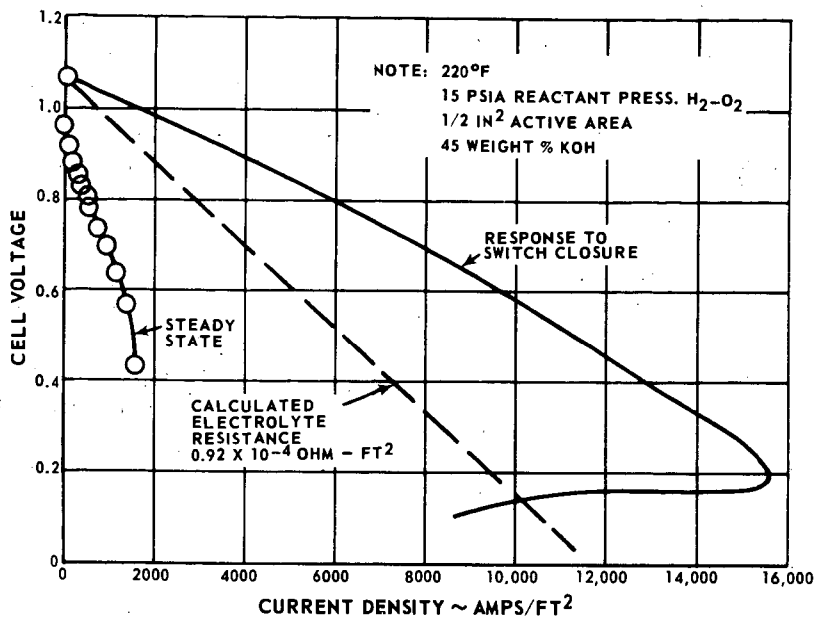


Figure 5 Trapped Electrolyte Cell Performance - Steady State and Transient

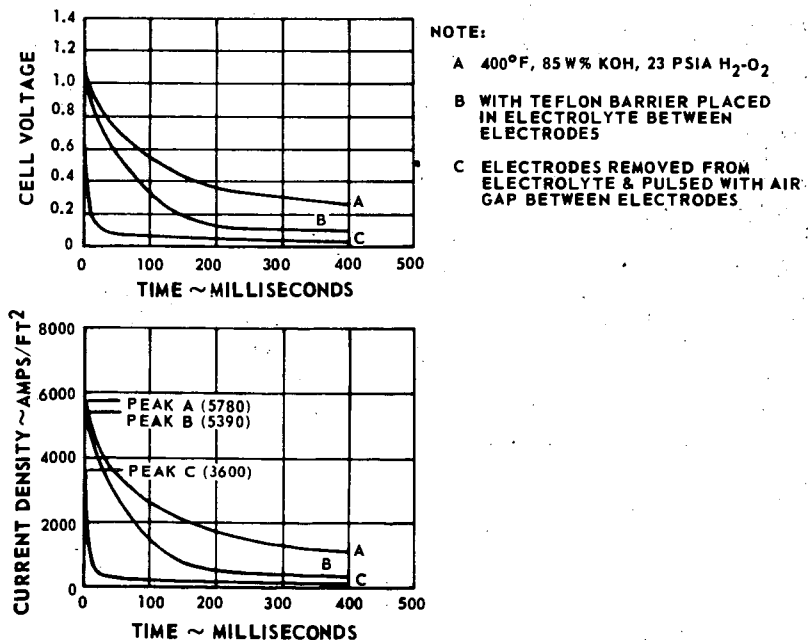


Figure 6 Free Electrolyte Cell - Millisecond Response

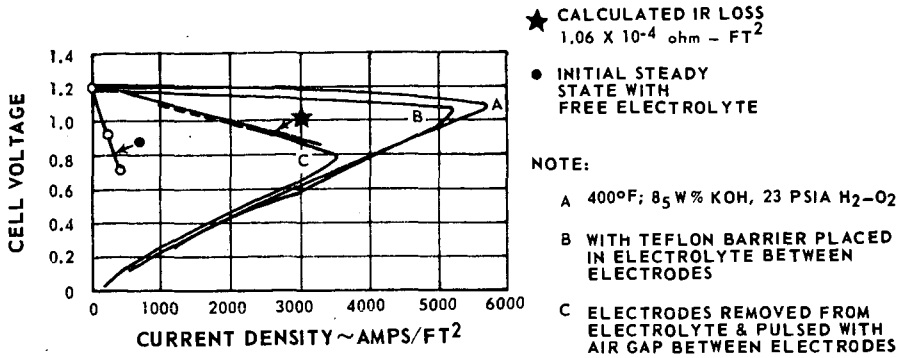


Figure 7 Free Electrolyte Cell - Performance Steady State and Transient

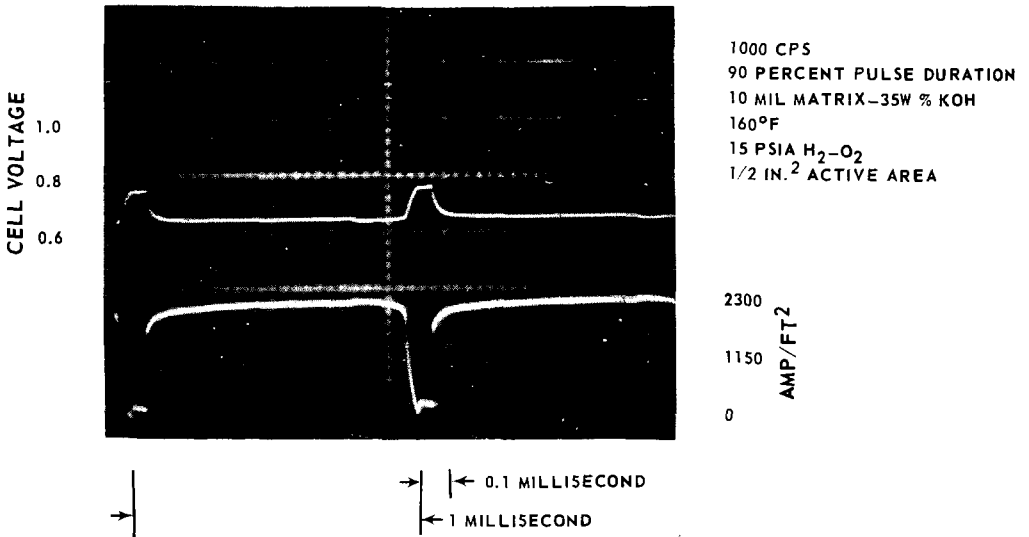


Figure 8 Trapped Electrolyte Cell Response to Repeated Pulse Loading

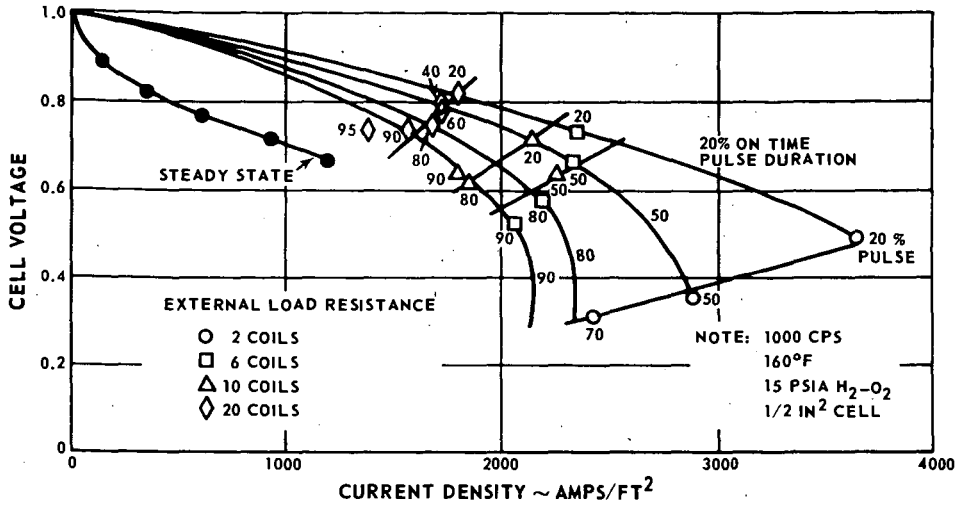


Figure 9 Trapped Electrolyte Cell Performance During Repeated Pulse Loading

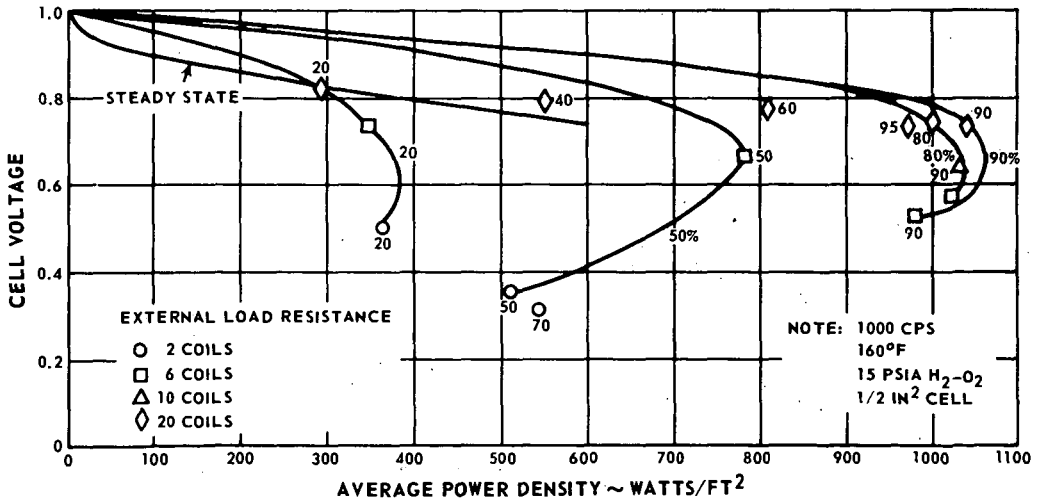


Figure 10 Trapped Electrolyte Cell - Average Power Density During Repeated Pulse Loading

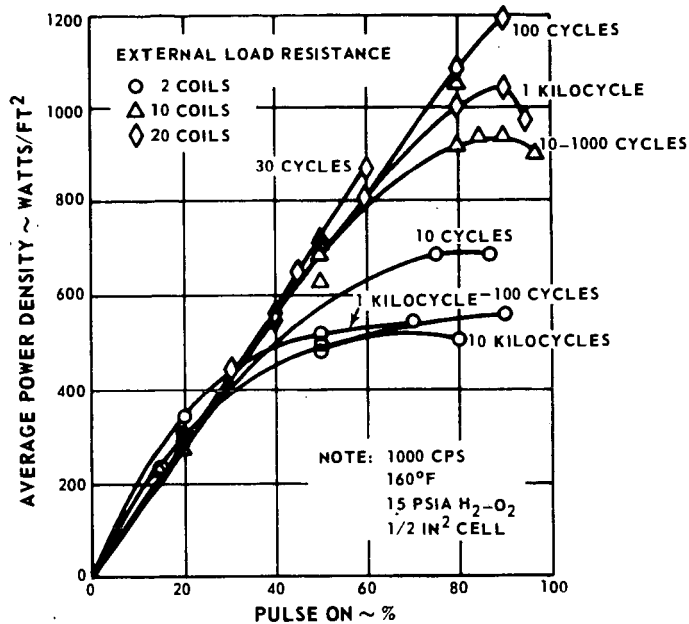


Figure 11 Trapped Electrolyte Cell - Effect of Pulse Duration and Frequency on Average Power Density

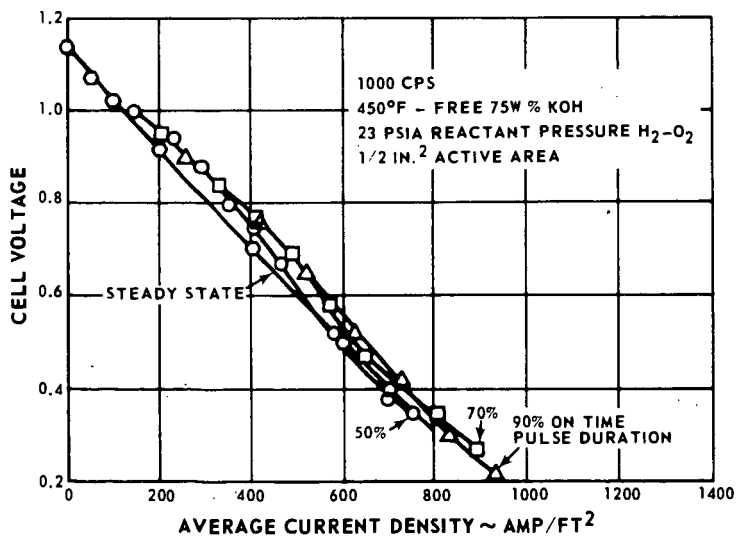


Figure 12 Free Electrolyte Cell - Average Performance During Repeated Pulse Loading

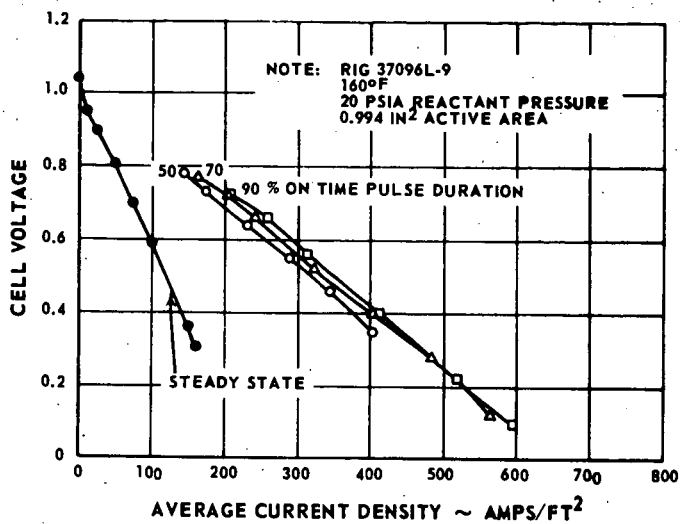


Figure 13 Low Temperature Free Electrolyte Effect of Repeated Pulsing on Performance